Computational Study of Sheath Structure in the Presence of Magnetic Field

T. Ibehej and R. Hrach

Charles University, Faculty of Mathematics and Physics, Prague, Czech Republic.

Abstract. The results of 2D particle and 3D particle/fluid hybrid simulations are presented. We investigated a plasma sheath formed near substrates of different shapes and showed the influence of magnetic field on the sheath structure and particle fluxes to the substrate. The studied solids were a cylindrical and a planar probe and a grooved planar substrate. The object of interest was idealized three-component plasma containing electrons and one species of positive and negative ions. This composition simulates frequently used plasma mixtures containing electronegative gas (e.g. oxygen or chlorine) and rare gas (e.g. argon). We used a simplified plasma composition to show general properties of electronegative plasmas interacting with solids. The effects of the presence of negative ions were investigated together with the effects of magnetic field. The simulations of plasma-solid interaction are useful not only for many plasma material treatment applications but also for an analysis of plasma probe diagnostics.

Introduction

The electronegative plasma containing negative ions has been intensively studied for long time theoretically (e.g. [*Franklin*, 2003, *Palop*, 2007]), experimentally [*Stoffels*, 1995] and computationally [*Sommerer*, 1992, *Gudmundsson*, 2002 and *Bleecker*, 2003]. The mixtures of electronegative and rare gases are widely used in many plasma-assisted material processing techniques, such as cleaning, etching, oxidizing, etc. In this contribution we studied the effects of uniform magnetic field during the interaction of electronegative plasma with solids. To show the influence of heavy negative species during the interaction, a positive bias was applied to the solid substrates. Simplified three-component plasma was simulated – as an example, we chose a mixture of argon and oxygen. The plasma contained electrons, one species of positive ions (Ar^+) and negative ions (O^-) together with one species of neutral particles for the needs of collisions.

Sufficiently detailed information of the studied system can be obtained with the particle technique of computational physics. We developed a two-dimensional Particle-In-Cell – Monte Carlo Collisions (PIC-MCC) model. Some of the results were verified by a fully three-dimensional particle/fluid simulation, which has significantly lower requirements of computational time, but it has certain limitations which are based on the limits of applicability of the used partial differential equations. The hybrid simulation is capable of providing less detailed results in comparison with the particle model.

Three different configurations of plasma-solid interaction were studied. The first one is the interaction of plasma with infinite cylindrical probe. The spatial distribution of electrostatic potential, particle densities and angular distributions of electron and ion fluxes to the probe were discussed. The second and third investigated configurations were an even planar substrate and a grooved substrate. The even substrate was used to compare the results in sufficiently large distance from the unevenness to ensure that the computational domain is large enough to cover the disturbance. In these configurations, we discussed the electron and O^- density distributions as well as the fluxes of electrons and ions to the surface of the substrate.

Description of the model

General electronegative plasma

The motion of particles was determined by three factors – the electrostatic field obtained from Poisson's equation, external uniform magnetic field and collisions with neutral background particles obtained from the Monte Carlo part of the simulation. The ratio of mean free path $\lambda = (n_g\sigma)^{-1}$ and Larmor radius $r_L = mv_\perp/eB$ can give us a rough guess at the magnetic field influence on the motion of particles. The magnitude of B was 0.1 T. For electron collisions we used the cross sections of Ar–e elastic collision, excitation to the $^3P_2$ level (11.55 eV) and ionization with threshold energy of 15.8 eV [*Phelps*,

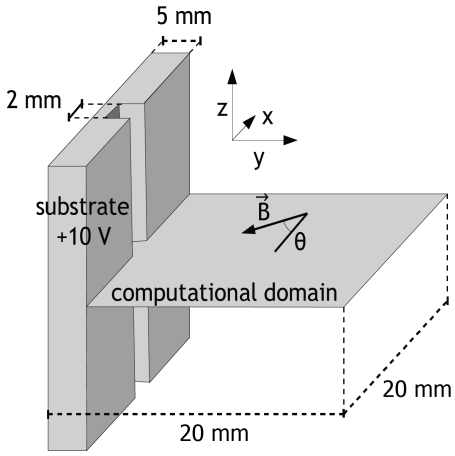

Figure 1. The third configuration of simulation representing a "grooved planar substrate."

2008]. Ar^+ collisions were Ar^+–Ar elastic collision and resonant charge exchange – both constants of $4.3{\cdot}10^{-15}$ cm^2 and $5.7{\cdot}10^{-15}$ cm^2. The last interaction, O^-–Ar elastic collision, has a slight energy dependency for our energy range, with mean value of $4.3{\cdot}10^{-15}$ cm^2. Table 1 shows the main parameters of the idealized Ar/O_2 plasma. The data in the table shows, that only electrons were strongly affected by the magnetic field. Both of the ion species moved without the influence of magnetic field, but it will be shown that they were influenced by the electric field formed by electrons.

Table 1. Parameters of the simplified electronegative three-component plasma.

	electrons	Ar^+	O^-	neutrals
density [m^{-3}]	$5{\cdot}10^{14}$	$1{\cdot}10^{15}$	$5{\cdot}10^{14}$	$3.22{\cdot}10^{22}$
mean energy [eV]	3.0 (23300 K)	0.039 (300 K)	0.039	0.039
total cross section [cm^2]	$4.2{\cdot}10^{-16}$	$8.6{\cdot}10^{-15}$	$4.3{\cdot}10^{-15}$	
mean free path [mm]	0.7	0.04	0.07	
Larmor radius [mm] ($B = 0.1$ T)	0.06	1.8	1.1	

Geometry of the model

The computational domain of the two-dimensional model was square-shaped with the side of 2 cm. In the first configuration a cylindrical probe with radius of 0.2 mm was located in the middle of the domain. On all boundaries of the domain the Dirichlet boundary conditions $U = 0$ V were applied. The particles which left the computational domain were discarded and the flux of particles from the undisturbed bulk plasma was realized by a source of particles – an independent model of the bulk plasma.

For the second configuration a planar substrate was located on one border of the computational domain. The source of particles was applied only on the opposite side of the domain and the boundary conditions on the perpendicular sides were periodical for both particles and electrostatic potential. The Figure 1 demonstrates the third configuration. The boundary conditions were the same as for the second configuration.

Computational properties

The presented model is a PIC-MCC simulation. The Poisson's equation was solved on a mesh of 400×400 nodes (configuration 1) and 500×500 nodes (configurations 2 and 3). A sparse system LU decomposition solver UMFPACK [*Davis*, 2004] was used. Collisions were simulated using a modified null collision method which takes into account the motion of collision targets [*Roucka*, 2011]. In the undisturbed plasma, a Maxwell distribution of charged particles was assumed. The motion of particles was computed using the velocity Verlet's method of second order of accuracy together with the HARHA (half acceleration – rotation – half acceleration) algorithm for magnetic field [*Birdsal*, 1991]. We used the OpenMP API for parallelization together with the gcc compiler. Our models are written in C language and were run on a workstation Xeon W3680 (6 cores, 3.33GHz, 24 GB RAM). It took about 1.5 day of computational time (with 10 million particles) to reach the stationary state and about 7 days to obtain smooth energy and angular distributions shown in following figures. The scalability of the code is demonstrated in Figure 2. With six threads in use, the execution time of one time step decreased by the

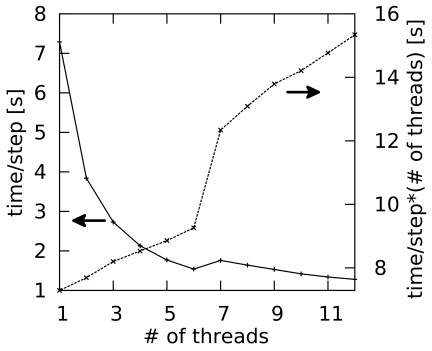

Figure 2. Computational requirements of the planar substrate simulation with 10 million particles.

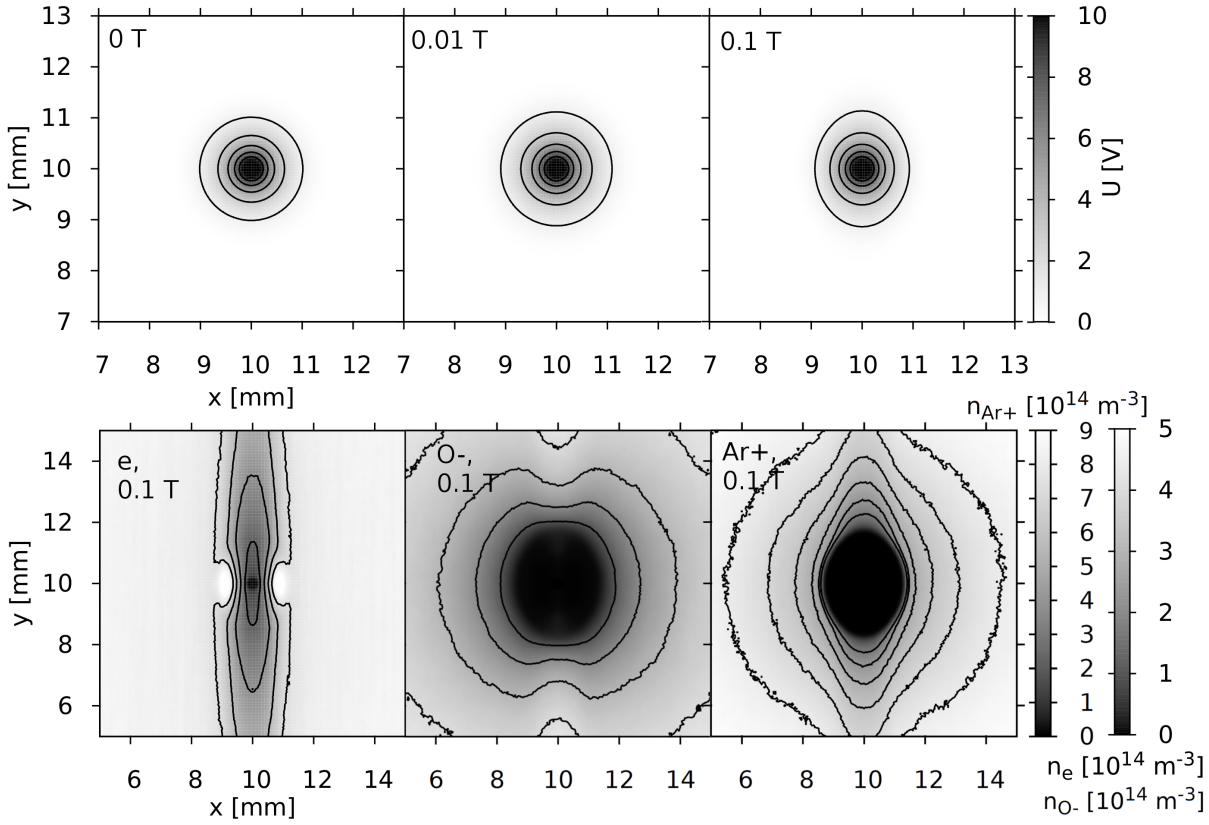

Figure 3. Magnetized electronegative sheath of the cylindrical probe. Top: Spatial distribution of the electrostatic potential for three different B. The values of the contour lines are (from outside) 1, 3, 5, 7 and 9 volts. Bottom: Densities of charged species for $B = 0.1$ T. Right colorbar relates to electrons and O^- ions, the contour lines (from outside) are 4, 3, 2 and 1 $\cdot 10^{14}$ m^{-3}. Left colorbar relates to Ar^+ ions, the range of contour lines is from 9 to 3 $\cdot 10^{14}$ m^{-3}.

factor of approximately 4.7. In addition, some computational time was eliminated by the hyperthreading technology resulting in the speed up of 5.7 with 6 cores physically available and all 12 threads in use.

Results and discussion

Cylindrical probe

The magnetic field of two different magnitudes was applied along y axis and the situation with no magnetic field was studied too. Figure 3 shows the structure of electronegative magnetized sheath. The deformation of the electrostatic potential at $B = 0.01$ T is negligible while at $B = 0.1$ T a slight deformation can be noticed. Nevertheless, the sheath was observed to be significantly deformed in terms of densities of charged particles. The diffusion profile of electrons at both 0.01 and 0.1 T changed

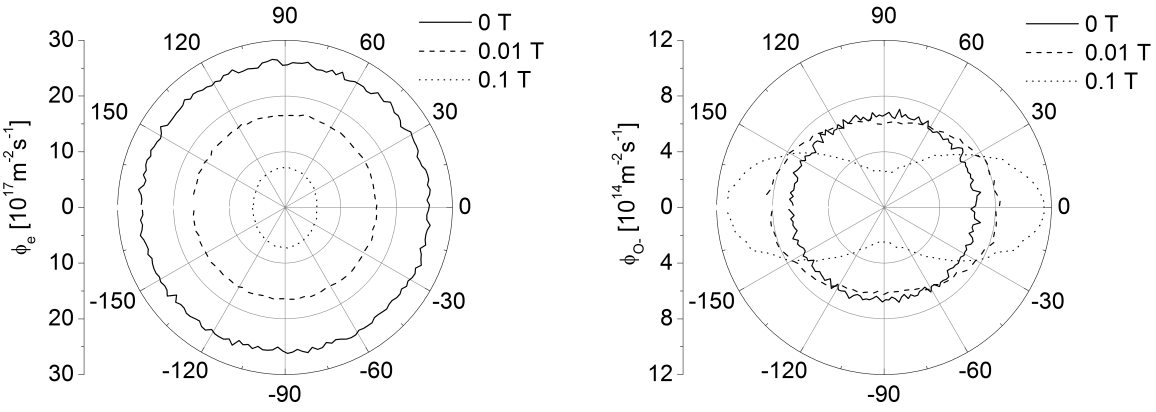

Figure 4. Angular distributions of electron (left) and O^- ion (right) fluxes to the cylindrical substrate for different B. $\varphi = 0°$ is parallel to $\vec{B}$.

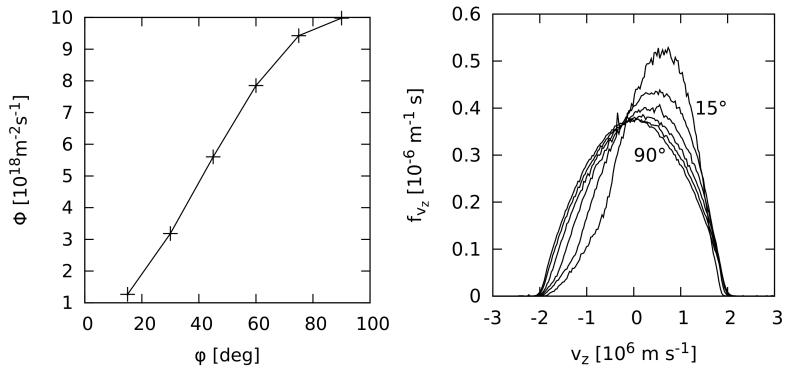

Figure 5. Left: increase of electron flux with increasing angle of $\vec{B}$. Right: demonstration of $\vec{E} \times \vec{B}$ drift, distribution of z velocity component for different directions of $\vec{B}$.

completely. At 0.1 T, the Larmor radius of electrons is smaller than their mean free path. In this case (Figure 3 left bottom) we observed, that the diffusion coefficient perpendicular to the magnetic field decreased and destroyed the typical logarithmic shape. Moreover, a maximum of electron densities can be found in the vicinity of the probe in perpendicular directions. This could be an effect of an electron trap formed by the potential of the probe and strong magnetic field. In the case of 0.01 T, the Larmor radius of electrons was comparable to their mean free path. The local maxima were not observed and the diffusion profile was wider.

An interesting situation was observed also for O^- ions which are affected by the magnetic field only negligibly. Therefore, they can substitute electrons in the regions where they cannot occur due to the magnetic field. The plasma quasineutrality can be satisfied in larger distances from the probe which leads to smaller deformation of potential profile. The substitution of O^- ions can be noted also at the fluxes to the probe (Figure 4). The trends of electrons and negative ions are inverse. We can also notice a significant decrease of electron flux with increasing magnetic field. This effect was treated both experimentally and theoretically [*Tagle*, 1987] in tokamak plasma and it was shown that the reduction of the electron current increases with decreasing mean free path and increasing size of the probe.

Planar and grooved substrate

The planar probe simulation was used mainly to validate the results of the third model which will be discussed further. As expected, we could observe an increase of electron and ion flux to the substrate with increasing angle of $\vec{B}$. At 90° the magnetic field was perpendicular to the probe, so the current reached its maximum (Figure 5 on the left). On the right side of Figure 5, we can observe the effect of $\vec{E} \times \vec{B}$ drift which reaches maximum at minimum angle. In this case, $\vec{B}$ and $\vec{E}$ created by the biased probe are perpendicular and the particles drift along z axis.

The influence of negative ions to the formation of sheath without magnetic field is discussed for the case of planar probe in our previous work [*Ibehej*, 2012].

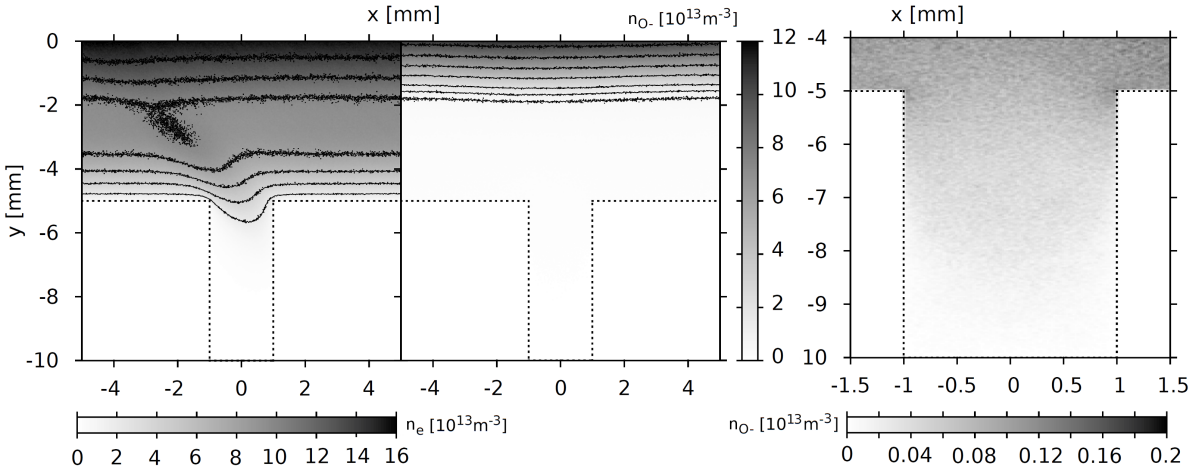

Figure 6. Magnetized electronegative sheath, $B = 0.1$ T, $\theta = 45°$. Left: Electron and O^- ion number densities in the vicinity of a groove with depth of 5 mm and width of 2 mm. Contour lines: electrons (2, 4, ... 16 $\cdot 10^{13}$ m^{-3}) and ions (0.5, 1, 2, 4, ... 10 $\cdot 10^{13}$ m^{-3}). Right: detailed view to the O^- ion number density in the groove.

The situation is more complex if the substrate is not even. As an example of uneven substrate, we have chosen a planar substrate with rectangular infinite groove. The width of the groove was 2 mm and depth 5 mm. The detailed view on the electronegative magnetized sheath formed near the substrate is available in Figure 6. The magnetic field with magnitude of 0.1 T was applied. Therefore, the motion of electrons was strongly influenced by the magnetic field. The deformation of ion density is not visible in Figure 6. Most of the ions were repelled by the substrate bias to the distance of 3 mm from the substrate. However, the right graph in Figure 6 shows some remaining O^- density which caused also very low flux of O^- to the substrate boundary.

The fluxes to the whole surface of the substrate are displayed in Figure 7. In the case of $\theta = 90°$, the electrons were able to penetrate to the bottom of the groove. Otherwise, electrons and ions reached a depth of several millimeters. The Figure 7 also shows the comparison with the iterative particle/fluid hybrid model. The fluid part of the model is based on numerical solution of Poisson's equation and continuity equations for every species. The vector flux of each species in the continuity equation is given by drift-diffusion approximation with magnetic field:

$$\begin{aligned}\vec{\Gamma}_k \;=\; & \left[\frac{q_k}{m_k\nu_k} n_k \vec{E} + \left(\frac{q_k}{m_k\nu_k}\right)^2 n_k \left(\vec{E}\times\vec{B}\right) + \left(\frac{q_k}{m_k\nu_k}\right)^3 n_k \left(\vec{E}\cdot\vec{B}\right)\vec{B} - \frac{1}{3\nu_k}\bar{v_k^2}\nabla n_k - \right. \\ & \left. - \frac{q_k}{m_k\nu_k}\cdot\frac{1}{3\nu_k}\bar{v_k^2}\left(\nabla n_k\times\vec{B}\right) - \left(\frac{q_k}{m_k\nu_k}\right)^2 \frac{1}{3\nu_k}\bar{v_k^2}\left(\nabla n_k\cdot\vec{B}\right)\vec{B}\right] \Big/ \left[1+\left(\frac{q_k B}{m_k\nu_k}\right)^2\right]. \qquad (1)\end{aligned}$$

The particle part is a non self-consistent particle model with collisions treated in the manner described above. The Figure 7 shows very good agreement. For ions, we had to use minor fitting factors of 1.2 and 1.5, respectively. This can be caused by the uncertain determination of absolute values of fluxes due to lower dimensionality of the PIC-MCC model.

Conclusion

We presented a simplified PIC-MCC model of electronegative plasma interacting with solids of different shapes in the presence of uniform magnetic field. The effects of collisions and magnetic field were discussed together with the effects of heavy negative ions. The sheath of the single cylindrical Langmuir probe was described in detail for magnetic field magnitude of 0, 0.01 and 0.1 T. We also described the interaction with positively biased uneven substrate and some results successfully compared with independent hybrid simulation. The capabilities of the model were presented on the simplified three-component plasma. However, the simulation is prepared to deal with more realistic plasmas both, electronegative and electropositive and various shapes of solids which satisfy the restrictions of two-dimensional model.

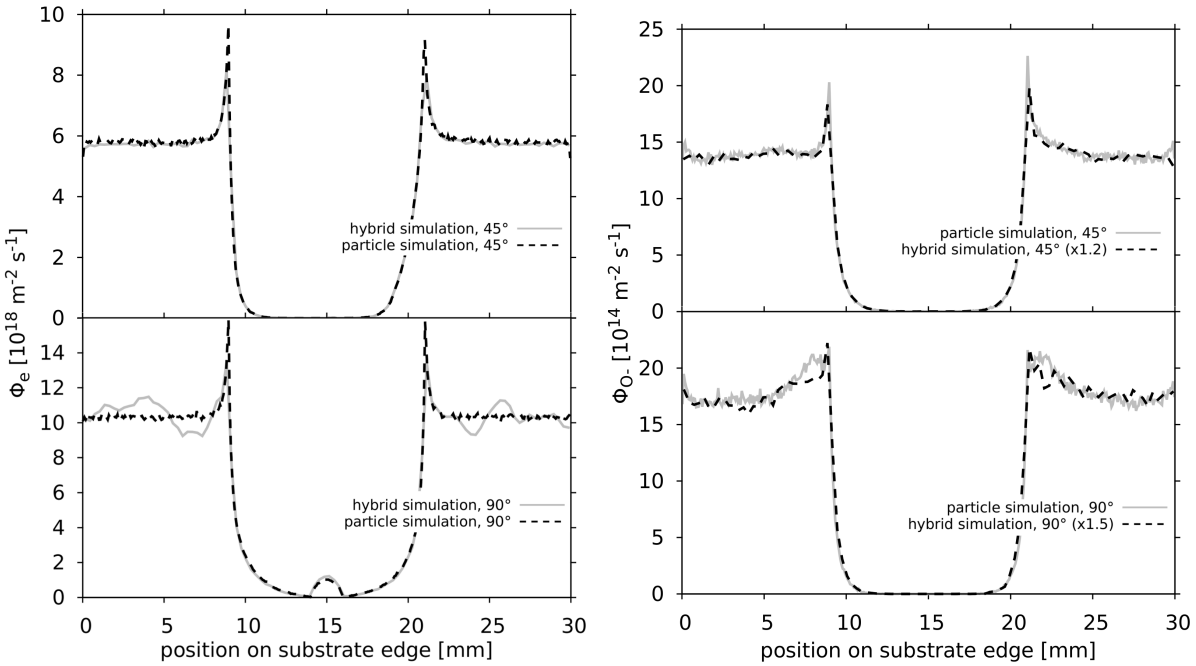

Figure 7. Fluxes of electrons (left) and O^- ions (right) to the grooved substrate. $B = 0.1$ T and $\theta = 45°$ (top) and $\theta = 90°$ (bottom). Comparison of PIC-MCC (particle) simulation with hybrid particle/fluid model.

Acknowledgment. The authors greatly acknowledge the support of the Grant Agency of Charles University (project 46310/2010) and the work and advice of our deceased colleague V. Hruby.

References

Birdsall, C. K., A. B. Langdon, *Plasma Physics via Computer Simulations*, Bristol, IOP Publishing, 1991.

Bleecker, K. D., D. Herrebout, A. Bogaerts, R. Gijbels and P. Descamps, One-Dimensional Modelling of a Capacitively Coupled RF Plasma in Silane/Helium, Including Small Concentrations of O_2 and N_2, *J. Phys. D: Appl. Phys.*, 36, 1826-1833, 2003.

Davis, T. A., Algorithm 832: UMFPACK v4.3 – An Unsymmetric-Pattern Multifrontal Method, *ACM T. Math. Software*, 30, 196-199, 2004.

Franklin, R. N., Electronegative Plasmas Diluted by Rare Gases, *J. Phys. D: Appl. Phys.*, 36, 2655-2659, 2003.

Gudmundsson, J. T., Global Model of Plasma Chemistry in a Low-Pressure O_2/F_2 discharge, *J. Phys. D: Appl. Phys.*, 35, 328-341, 2002.

Ibehej, T. and R. Hrach, Computational study of sheath structure for plasma-assisted technologies in the presence of electronegative plasma, *Vacuum*, 86, 1220-1222, 2012.

Palop, J. I. F., J. Ballesteros, M. A. Hernndez and R. M. Crespo, Sheath Structure in Electronegative Plasmas, *Plasma Sources Sci. Technol.*, 16, S76-S86, 2007.

Phelps, A. V., Compilation of Electron Cross Sections, online <http://jila.colorado.edu/~avp/collision_data/>, avalilable online on June 8th, 2012.

Roucka, S. and R. Hrach, Extending PIC Models to Higher Pressures – Enhanced Model of Collisions, *IEEE Trans. on Plasma Sci.*, 39, 3244-3250, 2011.

Sommerer, T. J. and M. J. Kushner, Numerical Investigation of the Kinetics and Chemistry of RF Glow Discharge Plasmas Sustained in He, N_2, O_2, $He/N_2/O_2$, $He/CF_4/O_2$ and SiH_4/NH_3 Using a Monte Carlo-Fluid Hybrid Model, *J. Appl. Phys.*, 71, 1654-1673, 1992.

Stoffels, E. et al., Negative Ions in a Radio-Frequency Oxygen Plasma, *Phys. Rev. E*, 51, 2425-2435, 1995.

Tagle, J. A., P. C. Stangeby and S. K. Erents, Errors in Measuring Electron Temperatures Using a Single Langmuir Probe in a Magnetic Field, *Plasma Phys. Control. Fusion*, 29, 297-301, 1987.